AUS | الجامعة الأميركية في الشارقة
American University of Sharjah

Efficiency in computing electrocardiology models

Youssef Belhamadia

Department of Mathematics and Statistics

American University of Sharjah

Go20 Conference on Scientific Computing and Software

May 22- 26, 2023, Gozo, Malta

Objectives

- Efficiency in computing the electrical wave of the heart.

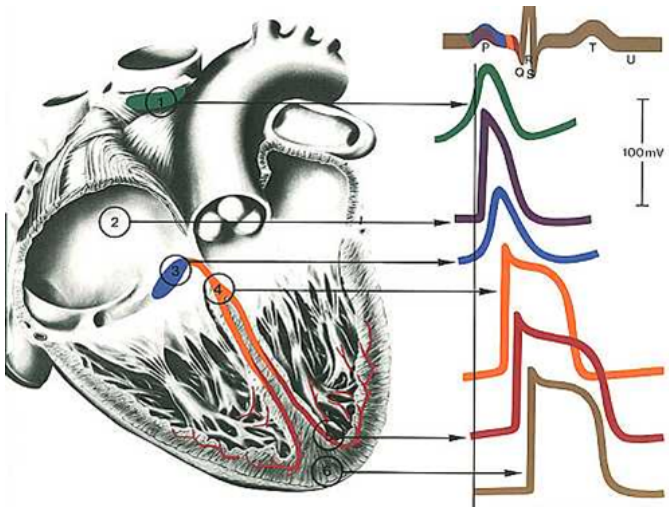

- Our goals :
  1. Introduce the Alternating Direction Implicit (ADI) method for solving the monodomain model.
  2. Derive a Semi-implicit Backward Differentiation ADI method for solving the Mitchell–Schaeffer Monodomain model.
  3. Investgate the efficiency of a parallel anisotropic mesh adaptation for solving electrocardiology models.

Hudgkin-Huxley 1952 (Noble Price 1962)

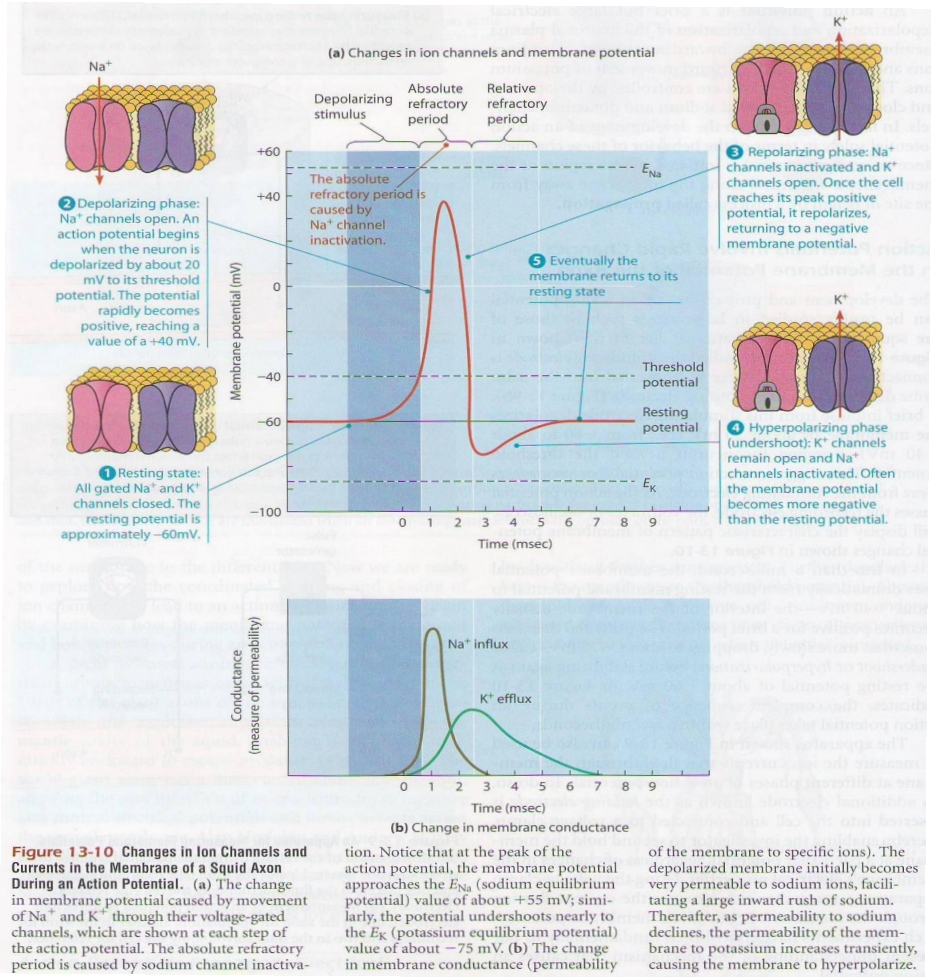

Figure 13-10 Changes in Ion Channels and Currents in the Membrane of a Squid Axon During an Action Potential. (a) The change in membrane potential caused by movement of Na^+ and K^+ through their voltage-gated channels, which are shown at each step of the action potential. The absolute refractory period is caused by sodium channel inactivation. Notice that at the peak of the action potential, the membrane potential approaches the E_{Na} (sodium equilibrium potential) value of about +55 mV; similarly, the potential undershoots nearly to the E_K (potassium equilibrium potential) value of about −75 mV. (b) The change in membrane conductance (permeability of the membrane to specific ions). The depolarized membrane initially becomes very permeable to sodium ions, facilitating a large inward rush of sodium. Thereafter, as permeability to sodium declines, the permeability of the membrane to potassium increases transiently, causing the membrane to hyperpolarize.

The World of the Cell, Wayne M. Becker et al., 7e édition.

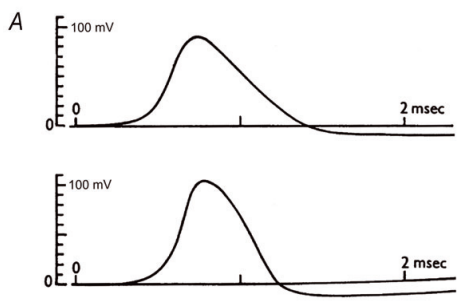

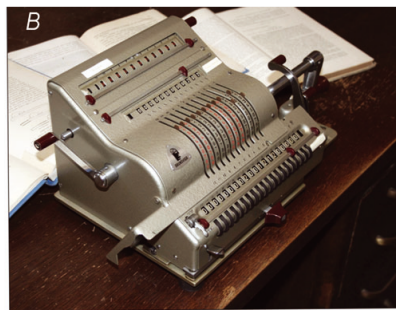

C. J. Schwiening, J. Physiol. 590.11 (2012) 2571–2575

Hodgkin-Huxley

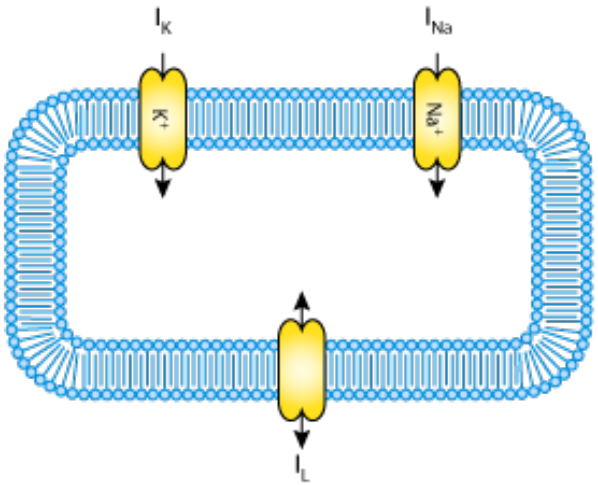

http ://www.cellml.org/

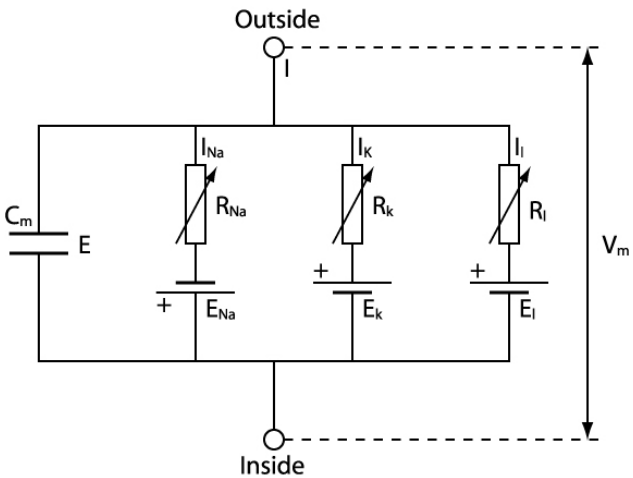

http ://alford.bios.uic.edu

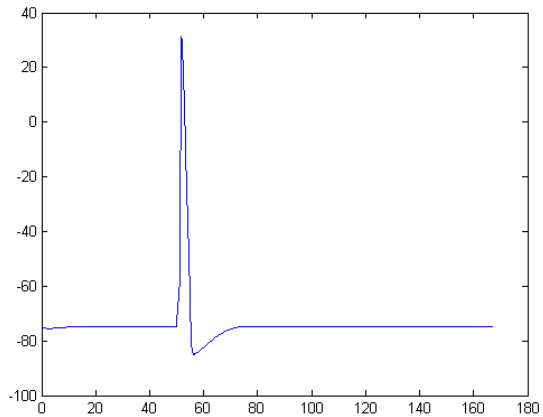

Potentiel transmembranaire

Ionic models

Luo Rudy I 1991 (9 ODE)*

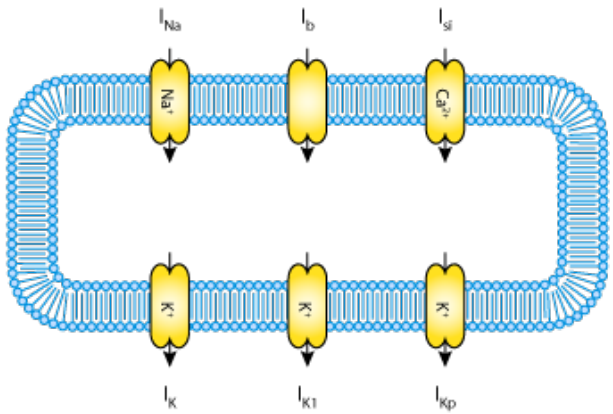

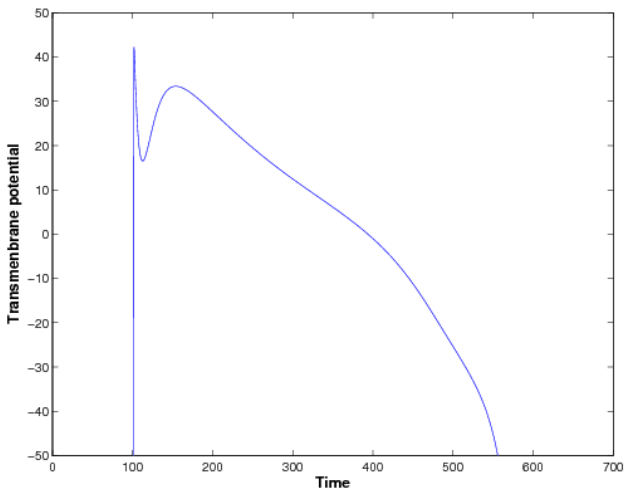

*http ://www.cellml.org/

Winslow 1999 (33 ODE)*

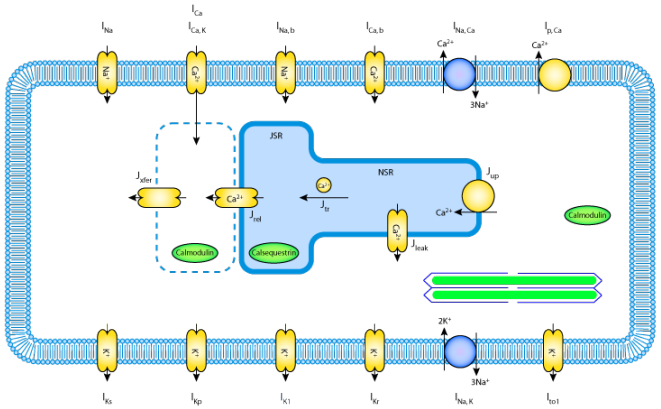

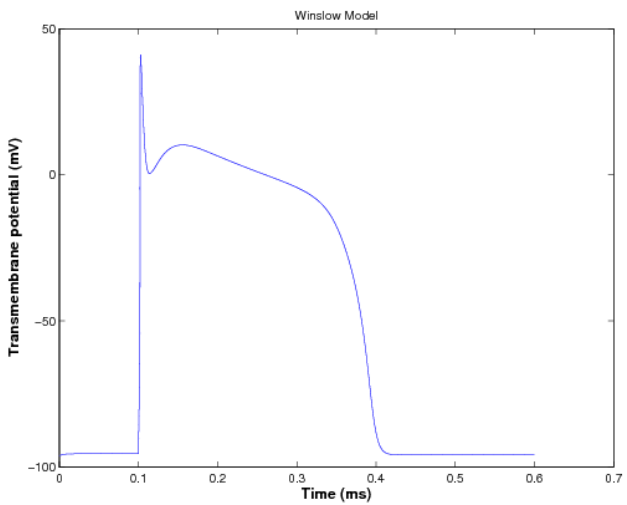

1. Solvers for ionic models :
   - Spiteri R.J. and Dean R.C., (2008) IEEE Trans Biomed Eng. 55(5) : 1488-95.
   - Sundnes J., Artebrant R., Skavhaug O. and Tveito A., (2009) IEEE Trans Biomed Eng. 56(10) : 2546-2548.
   - Marsh M. E., Ziaratgahi A. T., and Spiteri R. J., (2012) IEEE Trans Biomed Eng. 59(9) : 2506-2515
2. Simplified version of the ionic models : 2 variables
   - FitzHugh-Nagumo (1960-1961)
   - Aliev-Panfilov (1996)
   - Mitchell-Schaeffer (2004)

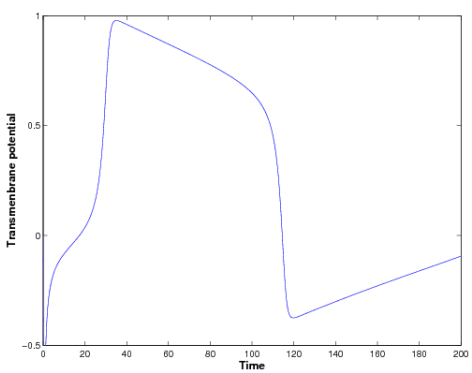

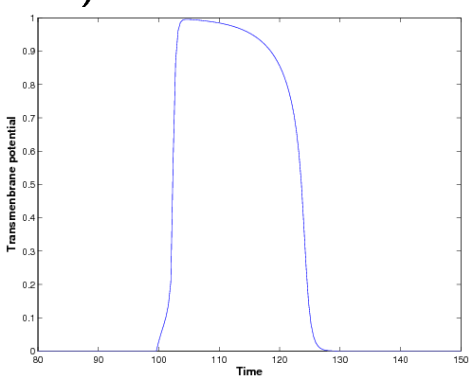

Bidomain model

- Proposed by Tung and Geselowitz (1978).
- $V_m = \phi_i - \phi_e$ transmembrane potential.
- ϕ_i intracellular potential.
- ϕ_e extracellular potential.
- W_n recovery variables.

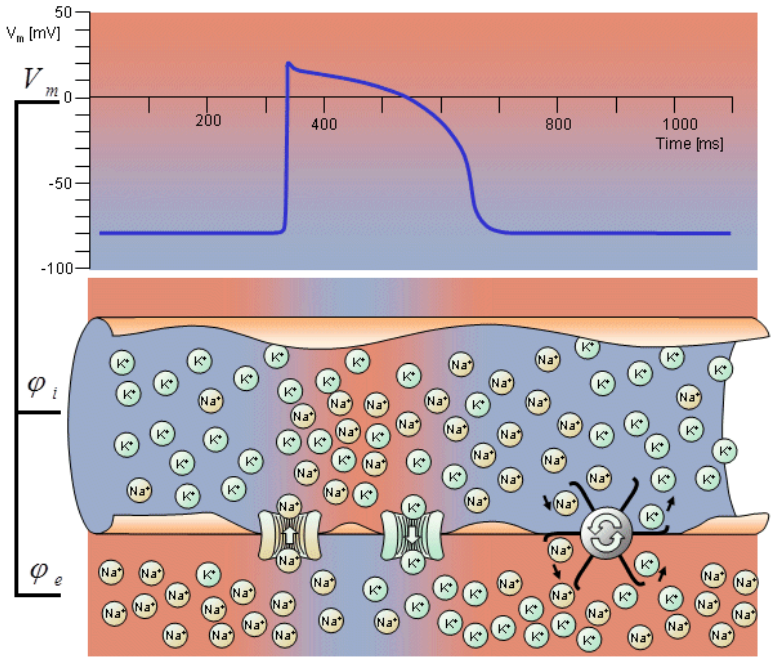

Bioelectromagnetism by Malmivuo and Plonsey

$$\frac{\partial V_m}{\partial t} - \nabla \cdot (\boldsymbol{G}_i \nabla V_m) = \nabla \cdot (\boldsymbol{G}_i \nabla \phi_e) + I_{ion}(V_m, W_n)$$

$$\nabla \cdot ((\boldsymbol{G}_i + \boldsymbol{G}_e) \nabla \phi_e) = -\nabla \cdot (\boldsymbol{G}_i \nabla V_m)$$

$$\frac{\partial W_n}{\partial t} = g(V_m, W_n),$$

The Monodomain Model

- The Bidomain Model can be simplified into the Monodomain Model by assuming that : $\boldsymbol{G}_i = \lambda \boldsymbol{G}_e$.
- Recall that the Bidomain *PDE* equations are :

$$\frac{\partial V_m}{\partial t} - \nabla \cdot (\boldsymbol{G}_i \nabla V_m) = \nabla \cdot (\boldsymbol{G}_i \nabla \phi_e) + I_{ion}(V_m, W_n)$$
$$\nabla \cdot ((\boldsymbol{G}_i + \boldsymbol{G}_e) \nabla \phi_e) = -\nabla \cdot (\boldsymbol{G}_i \nabla V_m)$$

- The second *PDE* becomes :

$$\nabla \cdot ((\lambda \boldsymbol{G}_e + \boldsymbol{G}_e) \nabla \phi_e) = -\nabla \cdot (\lambda \boldsymbol{G}_e \nabla V_m)$$

- Rearranging the terms gives :

$$\nabla \cdot (\boldsymbol{G}_e \nabla \phi_e) = -\frac{\lambda}{1+\lambda} \nabla \cdot (\boldsymbol{G}_e \nabla V_m)$$

- Plugging this result in the first *PDE* gives :

$$\frac{\partial V_m}{\partial t} = \frac{\lambda}{1+\lambda} \nabla \cdot (\boldsymbol{G}_e \nabla V_m) + I_{ion}(V_m, W_n)$$

Monodomain Model

- V_m represents the transmembrane potential.
- W_n represents the recovery variable which depends on the ionic model.

$$\begin{cases} \dfrac{\partial V_m}{\partial t} = & \nabla D \nabla V_m + I_{\text{ion}}(V_m, W_n) + I_s, \\ \dfrac{\partial W_n}{\partial t} = & G(V_m, W_n). \quad \forall n = 1 \cdots N. \end{cases}$$

- I_s is the current due to an external stimulus.
- The nonlinear reaction term $I_{\text{ion}}(V_m, W_n)$ and the function $G(V_m, W_n)$ depend on the ionic model.
- Ionic models accurately reproduce the most of the basic proprieties of cardiac tissue.

Ionic Models

- Mitchell–Schaeffer ionic model

$$I_{ion}(V_m, W) = \frac{1}{\tau_{in}} W V^2 (1 - V) - \frac{1}{\tau_{out}} V,$$

$$G(V_m, W) = \begin{cases} \dfrac{1 - W}{\tau_{open}} & \text{for} \quad V < v_{gate}, \\ -\dfrac{W}{\tau_{close}} & \text{for} \quad V \geq v_{gate}. \end{cases}$$

- Reproduce more realistic shape of the cardiac action potential.
- Reproduce the APD restitution characteristic observed in the experiments.
- The simulations results could be compared to experimental studies.

Computational Challenges :

- Rapid dynamics of the cellular reactions described by the system of *ODEs* and the ionic term introduced in the *PDE*.
- Necessity of a high resolution space and time discretization.
- The coupling between the *PDEs* and the system of *ODEs*.

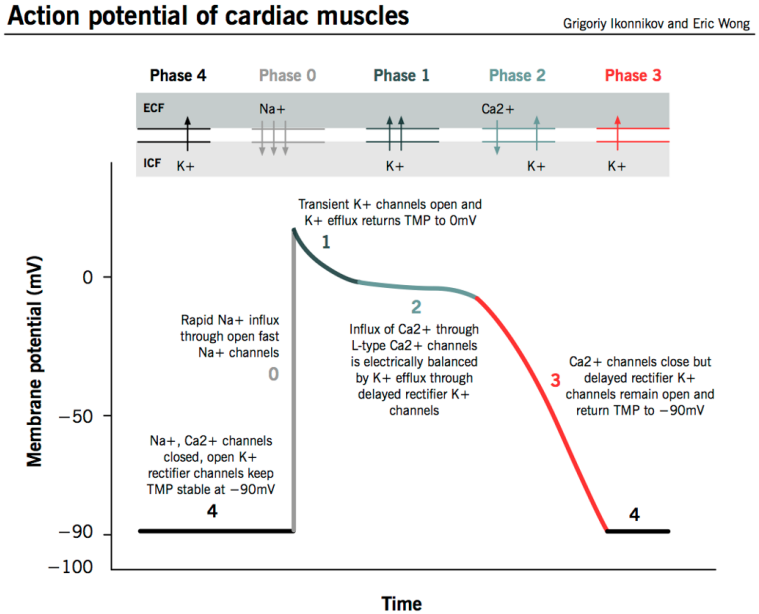

http ://www.pathophys.org/physiology-of-cardiac-conduction-and-contractility/

Methods for Numerical Discretization

Time Discretization Methods :

- Semi-implicit methods
- Fully implicit methods
- Operator splitting methods

Space Discretization Methods :

- Uniform and non-uniform meshes
- Adapted meshes

Semi-implicit Methods

- **First Order Methods :**
  forward Euler, forward-backward Euler, Crank-Nicolson-forward Euler, IMEX first order Gear, backward Euler.
- **Second Order Methods :**
  Crank-Nicolson/Adams-Basforth, modified Crank-Nicolson/Adams-Basforth, second-order semi-implicit backward differentiation (*SBDF*), implicit gear.
- **Third Order Methods :**
  Third order *SBDF*.

The semi-implicit methods (CNAB and SBDF) are among the best schemes available to solve the cardiac models.

1. M. Ethier and Y. Bourgault, **Semi-Implicit Time Discretization Schemes for the Bidomain Model**, SIAM : Journal on Numerical Analysis, vol. 46, pp. 2443-2468, 2008.
2. T Roy, Y Bourgault, C Pierre **Analysis of time-stepping methods for the monodomain model.** Computational and Applied Mathematics 39 (3), 1-32, 2020.

Finite Difference Method

$$\begin{cases} \dfrac{\partial V_m}{\partial t} - \nabla \cdot (\boldsymbol{D} \nabla V_m) &= I_{ion}(V_m, \boldsymbol{W}), \\ \dfrac{\partial \boldsymbol{W}}{\partial t} &= g(V_m, \boldsymbol{W}). \end{cases}$$

$$\frac{\partial \boldsymbol{U}}{\partial t} = A\boldsymbol{U} + F(\boldsymbol{U}),$$

where

$$\boldsymbol{U} = \begin{pmatrix} V \\ \boldsymbol{W} \end{pmatrix}, \quad A = \begin{pmatrix} D_x \dfrac{\partial^2}{\partial x^2} + D_y \dfrac{\partial^2}{\partial y^2} & \mathbf{0} \\ \mathbf{0} & \mathbf{0} \end{pmatrix}$$

and

$$F(\boldsymbol{U}) = \begin{pmatrix} I_{ion}(V, \boldsymbol{W}) \\ g(V, \boldsymbol{W}) \end{pmatrix}.$$

Crank-Nicolson/Adams-Bashforth Method

Crank–Nicolson/Adams–Bashforth (CNAB)

$$\frac{\boldsymbol{U}^{n+1}-\boldsymbol{U}^{n}}{\Delta t}+\frac{1}{2}A\boldsymbol{U}^{n+1}+\frac{1}{2}A\boldsymbol{U}^{n}=\frac{3}{2}F(\boldsymbol{U}^{n})-\frac{1}{2}F(\boldsymbol{U}^{n-1}).$$

1. Peacema–Rachford ADI-type method
2. Douglas–Gunn ADI-type method
3. and D'Yakonov ADI-type method

Belhamadia Y., and Rammal Z. (2021), Efficiency of Semi-Implicit Alternating Direction Implicit Methods for Solving Cardiac Monodomain Model. Computers in Biology and Medicine. DOI : https ://doi.org/10.1016/j.compbiomed.2020.104187

Semi-Implicit-Backward Difference

1. Semi-Implicit-Backward Difference formula of order 2 :

$$\frac{3\boldsymbol{U}^{n+1} - 4\boldsymbol{U}^{n} + \boldsymbol{U}^{n-1}}{\Delta t} = A\boldsymbol{U}^{n+1} + 2F^{n} - F^{n-1}$$

2. Semi-Implicit-Backward Difference formula of order 3 :

$$\frac{\frac{11}{6}\boldsymbol{U}^{n+1} - 3\boldsymbol{U}^{n} + \frac{3}{2}\boldsymbol{U}^{n-1} - \frac{1}{3}\boldsymbol{U}^{n-2}}{\Delta t} = A\boldsymbol{U}^{n+1} + 3F^{n} - 3F^{n-1} + F^{n-2}$$

3. Semi-Implicit-Backward Difference formula of order 4 :

$$\frac{\frac{25}{12}\boldsymbol{U}^{n+1} - 4\boldsymbol{U}^{n} + 3\boldsymbol{U}^{n-1} - \frac{4}{3}\boldsymbol{U}^{n-2} + \frac{1}{4}\boldsymbol{U}^{n-3}}{\Delta t} = A\boldsymbol{U}^{n+1} + 4F^{n} - 6f^{n-1} + 4F^{n-2} - F^{n-3}$$

SBDF-ADI

$$\frac{3\boldsymbol{U}^{n+1} - 4\boldsymbol{U}^{n} + \boldsymbol{U}^{n-1}}{2\Delta t} = A\boldsymbol{U}^{n+1} + 2F(\boldsymbol{U}^{n}) - F(\boldsymbol{U}^{n-1})$$

$$\frac{3\boldsymbol{U}^{n+1} - 4\boldsymbol{U}^{n} + \boldsymbol{U}^{n-1}}{2\Delta t} = A_1\boldsymbol{U}^{n+1} + A_2\boldsymbol{U}^{n+1} + 2F(\boldsymbol{U}^{n}) - F(\boldsymbol{U}^{n-1}) \quad (1)$$

where

$$A_1 = \begin{pmatrix} D_x \dfrac{\partial^2}{\partial x^2} & \mathbf{0} \\ \mathbf{0} & \mathbf{0} \end{pmatrix} \text{ and } A_2 = \begin{pmatrix} D_y \dfrac{\partial^2}{\partial y^2} & \mathbf{0} \\ \mathbf{0} & \mathbf{0} \end{pmatrix}.$$

SBDF-ADI

Rearanging (1) by taking $\boldsymbol{U}^{n+1}$ terms in one side and the rest terms in the other :

$$\left(I - \frac{2\Delta t}{3}A_1 - \frac{2\Delta t}{3}A_2\right)\boldsymbol{U}^{n+1} = \frac{4}{3}\boldsymbol{U}^n - \frac{1}{3}\boldsymbol{U}^{n-1} + \frac{2\Delta t}{3}\left(2F(\boldsymbol{U}^n) - F(\boldsymbol{U}^{n-1})\right). \tag{2}$$

The main idea for ADI is to use a perturbation of this equation. In our case, the perturbed form used is

$$\left(I - \frac{2\Delta t}{3}A_1\right)\left(I - \frac{2\Delta t}{3}A_2\right)\boldsymbol{U}^{n+1} = \frac{4}{3}\boldsymbol{U}^n - \frac{1}{3}\boldsymbol{U}^{n-1} + \frac{2\Delta t}{3}\left(2F(\boldsymbol{U}^n) - F(\boldsymbol{U}^{n-1})\right) \tag{3}$$

Both equations, (2) and (3), are equivalent and preserve the same time order of accuracy.

SBDF-ADI

Now, based on the Douglas–Gunn time splitting scheme, our proposed SBDF-ADI scheme consists of the following system of equations :

$$\begin{cases} \left(I - \frac{2\Delta t}{3} A_1\right) \boldsymbol{U}^* = \frac{\Delta t}{3} A_2 \boldsymbol{U}^n + \frac{4}{3}\boldsymbol{U}^n - \frac{1}{3}\boldsymbol{U}^{n-1} + \frac{2\Delta t}{3}\left(2F(\boldsymbol{U}^n) - F(\boldsymbol{U}^{n-1})\right), \\ \left(I - \frac{2\Delta t}{3} A_2\right) \boldsymbol{U}^{n+1} = \boldsymbol{U}^* - \frac{2\Delta t}{3} A_2 \boldsymbol{U}^n. \end{cases}$$

Alqasemi M. and Belhamadia Y. (2021), A Semi-implicit Backward Differentiation ADI Method for Solving Monodomain Model. Lecture Notes in Computer Science series. Part V, Volume 12746.

Evolution of the Transmembrane Potential

Table – Parameters used in Mitchell–Schaeffer model

Constant	Value	Constant	Value
τ_{in}	0.05	τ_{out}	1
τ_{open}	95	τ_{close}	162
v_{gate}	0.13(mV)	$D_x = D_y$	0.001

$$e_{L^\infty} = \|V_h - V_r\|_{L^\infty} \text{ and } e_{L^2} = \|V_h - V_r\|_{L^2},$$

where V_r is a reference solution for the transmembrane potential obtained with a spatial discretization of 401 points ($M = 400$) in each direction and small time step ($N = 2 \times 10^6$). V_h is the numerical solution obtained with the same spatial mesh. In this example, the final time is $T = 330$.

Evolution of the Transmembrane Potential

Evolution of the Transmembrane Potential

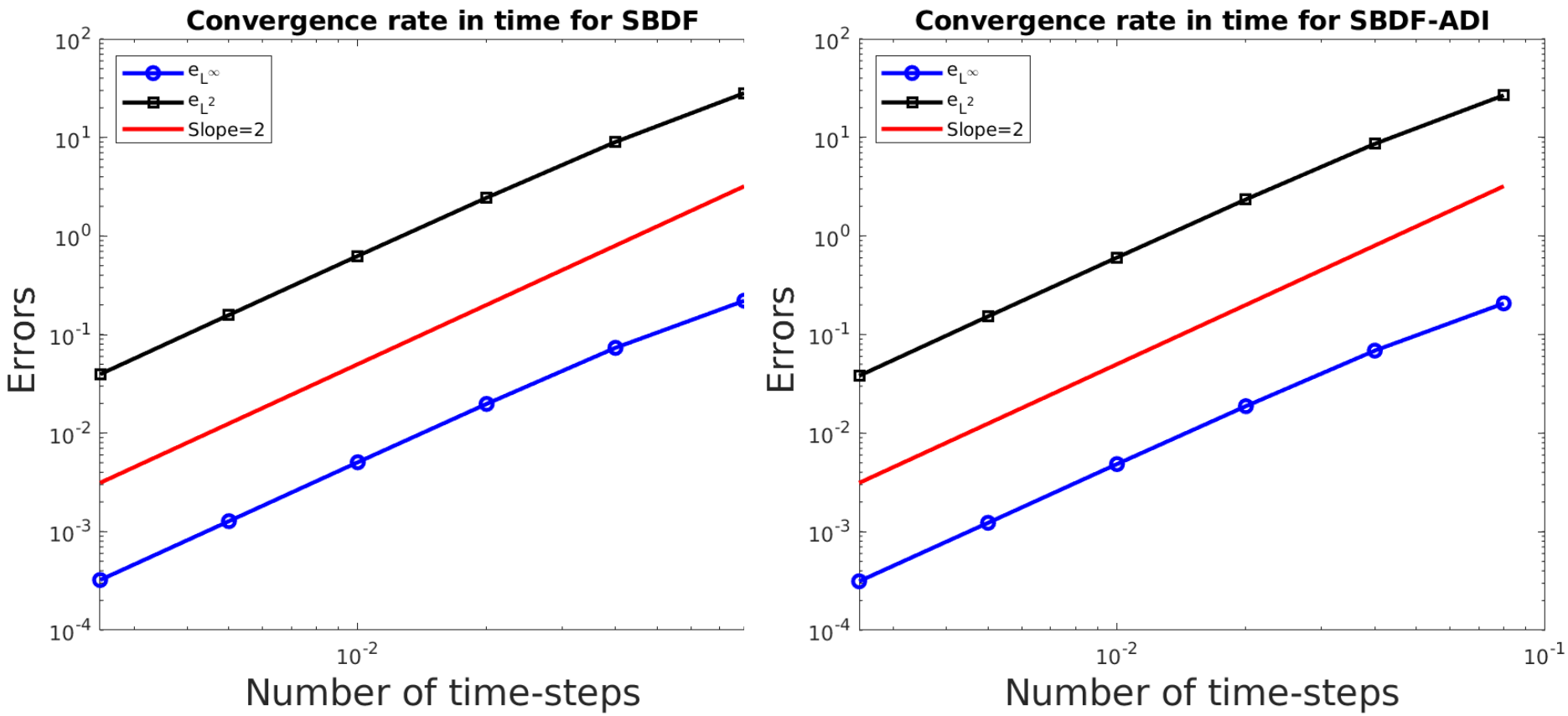

Figure – Convergence order for SBDF and SBDF-ADI using Mitchell–Schaeffer model.

Evolution of the Transmembrane Potential

Run Time Comparison

- The computational time for the SBDF-ADI method is very small compared to standard finite different methods (SBDF).
- ADI method allows the use of fine space discretization.
- The rapid results provided by the SBDI-ADI is a powerful advantage for electrocardiology models.

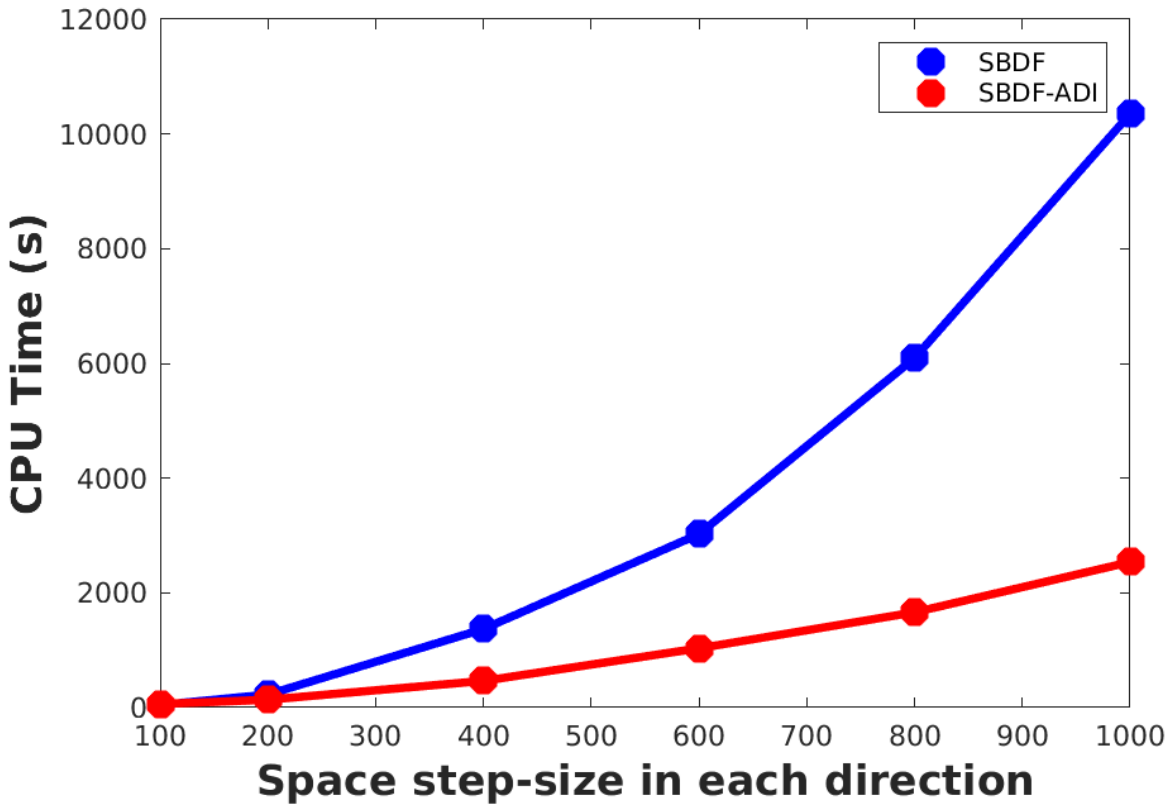

3D-ADI

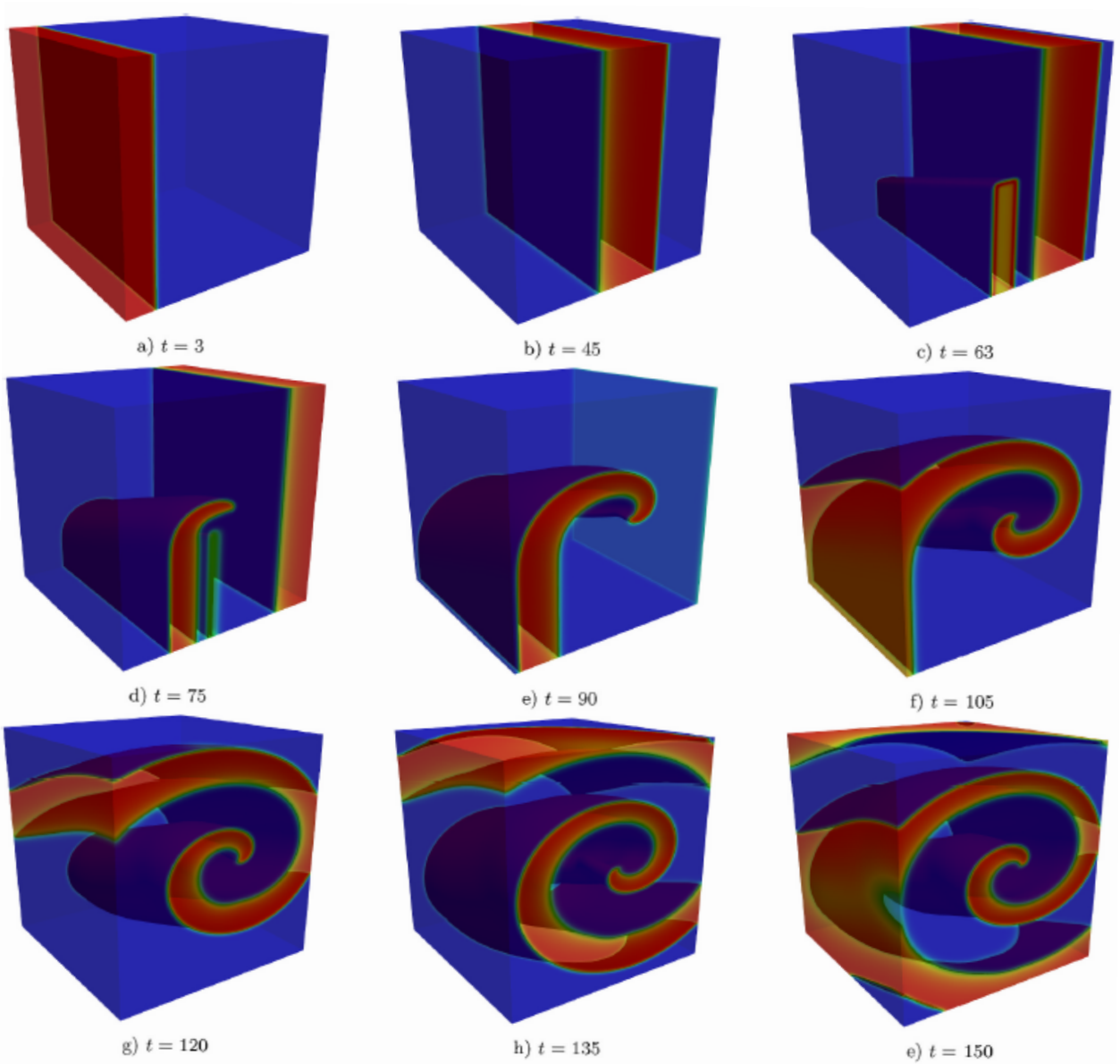

Memory Consumption

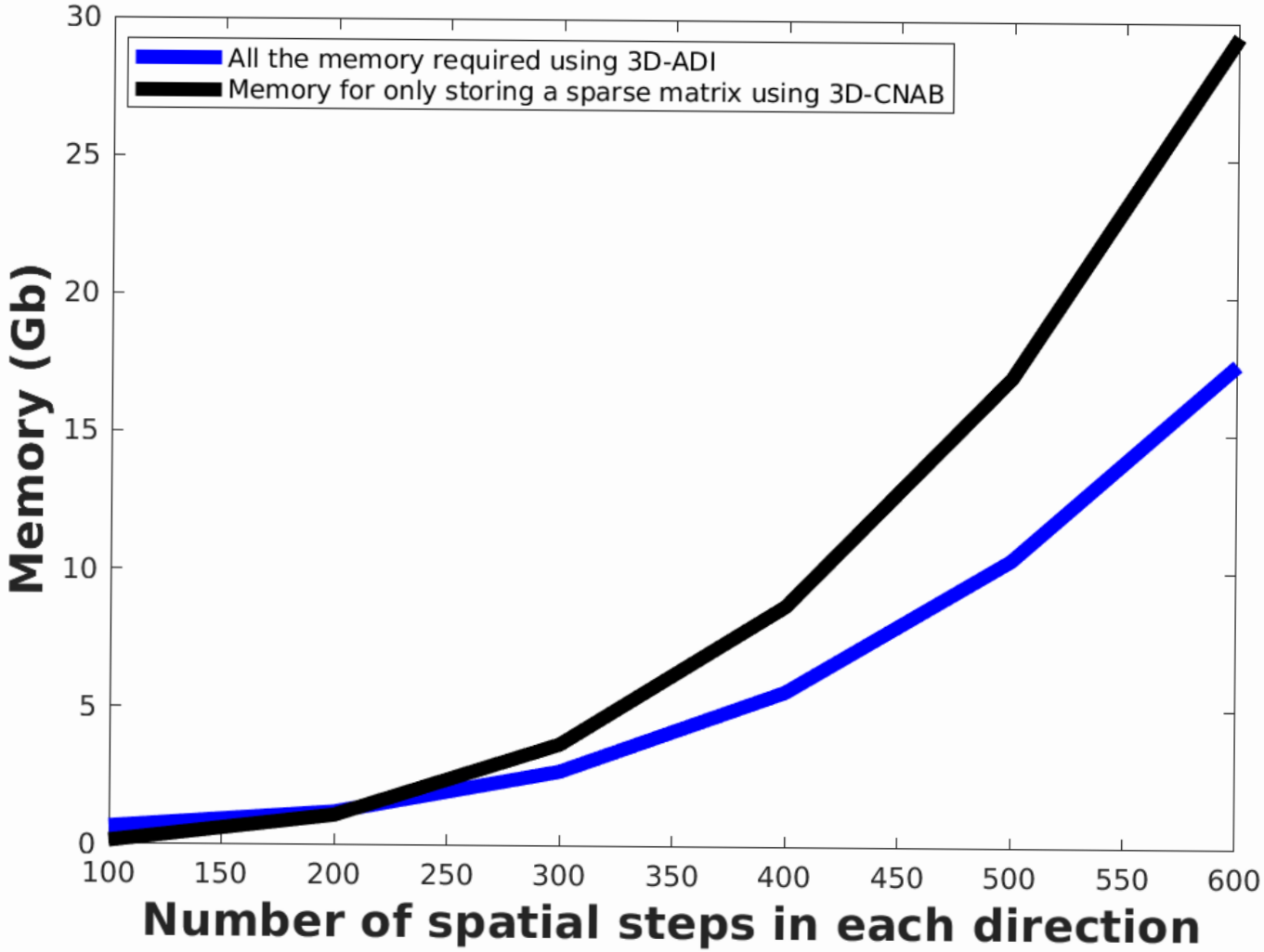

Conclusions and Future Work

- ADI algorithm speeds up the run-time over the most used methods for electro-cardiology models.
- ADI method reduces also the memory usage.
- SBDF-ADI can be extended to higher order time and space methods.
- The reduction in computational resources with SBDF-ADI method are significant in 3D.
- **Future Work :** Consider the bidomain model, consider the full tensor for the conductivity, consider realistic ionic models

Bidomain model

- Proposed by Tung and Geselowitz (1978).
- $V_m = \phi_i - \phi_e$ transmembrane potential.
- ϕ_i intracellular potential.
- ϕ_e extracellular potential.
- W_n recovery variables.

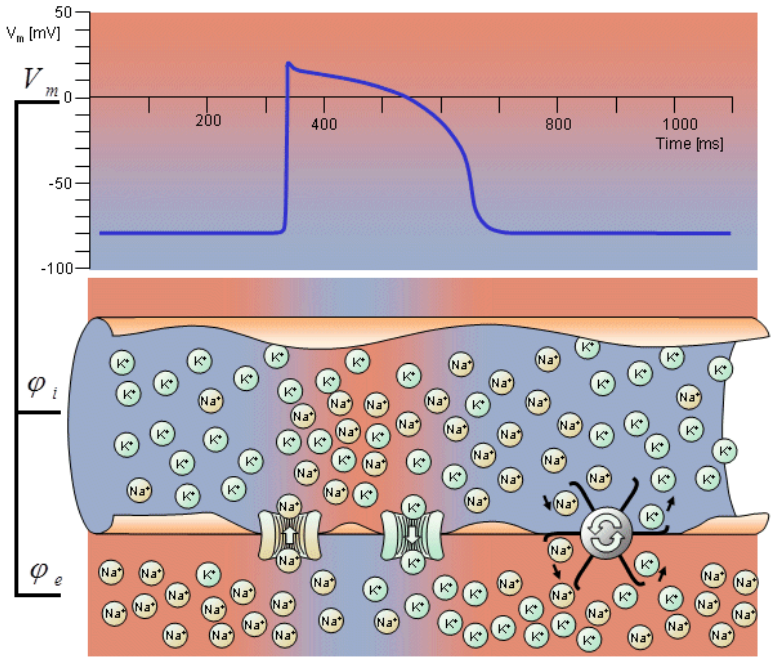

Bioelectromagnetism by Malmivuo and Plonsey

$$\frac{\partial V_m}{\partial t} - \nabla \cdot (\boldsymbol{G}_i \nabla V_m) = \nabla \cdot (\boldsymbol{G}_i \nabla \phi_e) + I_{ion}(V_m, W_n)$$

$$\nabla \cdot ((\boldsymbol{G}_i + \boldsymbol{G}_e) \nabla \phi_e) = -\nabla \cdot (\boldsymbol{G}_i \nabla V_m)$$

$$\frac{\partial W_n}{\partial t} = g(V_m, W_n),$$

Variational formulation

$$\int_\Omega \frac{3V_m^{(n+1)} - 4V_m^{(n)} + V_m^{(n-1)}}{2\Delta t}\,\psi_v\,d\Omega + \int_\Omega \boldsymbol{G}_i \boldsymbol{\nabla} V_m^{(n+1)} \cdot \boldsymbol{\nabla}\psi_v\,d\Omega$$

$$+ \int_\Omega \boldsymbol{G}_i \boldsymbol{\nabla} \phi_e^{(n+1)} \cdot \boldsymbol{\nabla}\psi_v\,d\Omega = \int_\Omega I_{ion}(V_m^{(n+1)}, W^{(n+1)})\psi_v\,d\Omega$$

$$- \int_\Omega (\boldsymbol{G}_i + \boldsymbol{G}_e)\boldsymbol{\nabla}\phi_e^{(n+1)} \cdot \boldsymbol{\nabla}\psi_\phi\,d\Omega = \int_\Omega \boldsymbol{G}_e \boldsymbol{\nabla} V_m^{(n+1)} \cdot \boldsymbol{\nabla}\psi_\phi\,d\Omega$$

$$\int_\Omega \frac{3W^{(n+1)} - 4W^{(n)} + W^{(n-1)}}{2\Delta t}\psi_w\,d\Omega = \int_\Omega g(V_m^{(n+1)}, W^{(n+1)})\,\psi_w\,d\Omega.$$

- Newton's method for the nonlinear equations.
- Implicit Euler, Crank Nicholson and Gear scheme for the time discretization.

Heart geometry*

Regular mesh, 205418 dofs

Adapted mesh, 96000 dofs

*Belhamadia Y., Fortin A. and Bourgault Y. (2009), Mathematical Biosciences. 220(2) : 89-101.

Heart geometry*

Parallel Anisotropic mesh adaptation

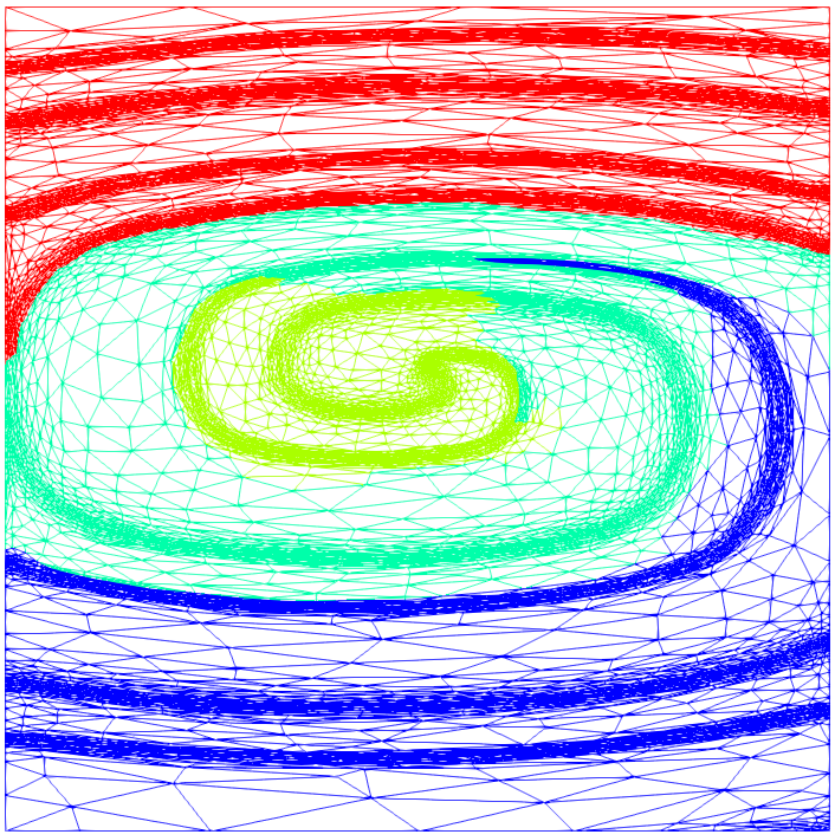

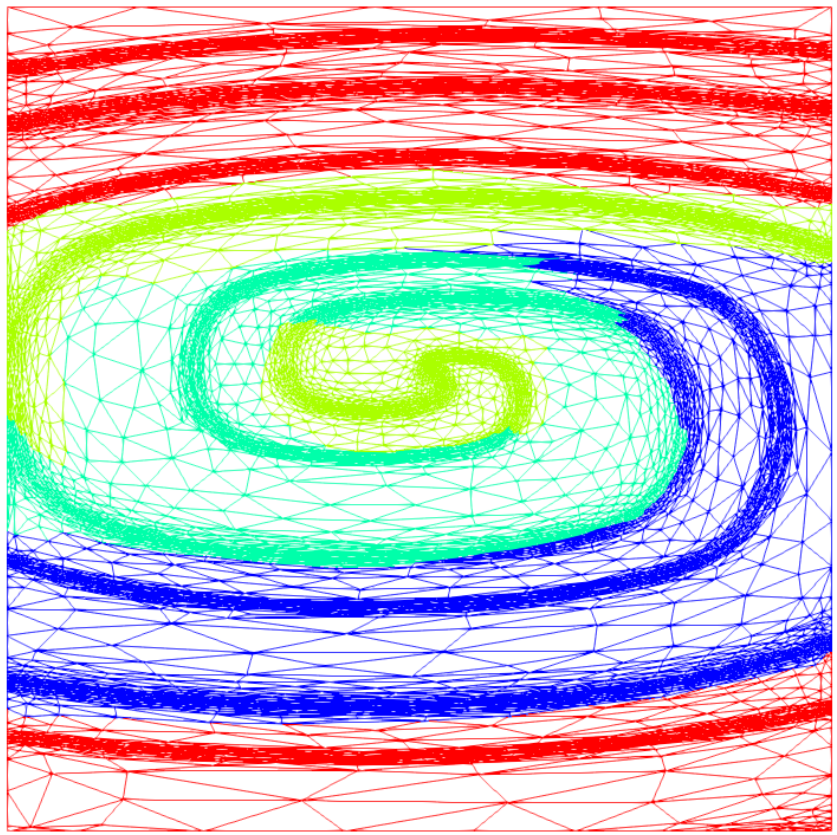

Parallel Anisotropic mesh adaptation

$$E_2(t = 500) = \frac{\|V^h - V^{ref}\|_2}{\|V^{ref}\|_2} \times 100\%$$

Table – Comparison of number of triangles and the error E_2 obtained with the parallel adapted and uniform meshes using 8, 16 and, 32 processors.

Parallel Uniform Meshes				
# triangles	E_2	CPU per step 8 processors	CPU per step 16 processors	CPU per step 32 processors
80000	37.98%	0.1min	0.07min	0.04min
320000	4.49%	0.44min	0.27min	0.18min
Parallel Adapted Meshes				
11 300	3.65%	0.26min	0.19min	0.16min
16 000	1.52%	0.37min	0.25min	0.19min

Heart geometry

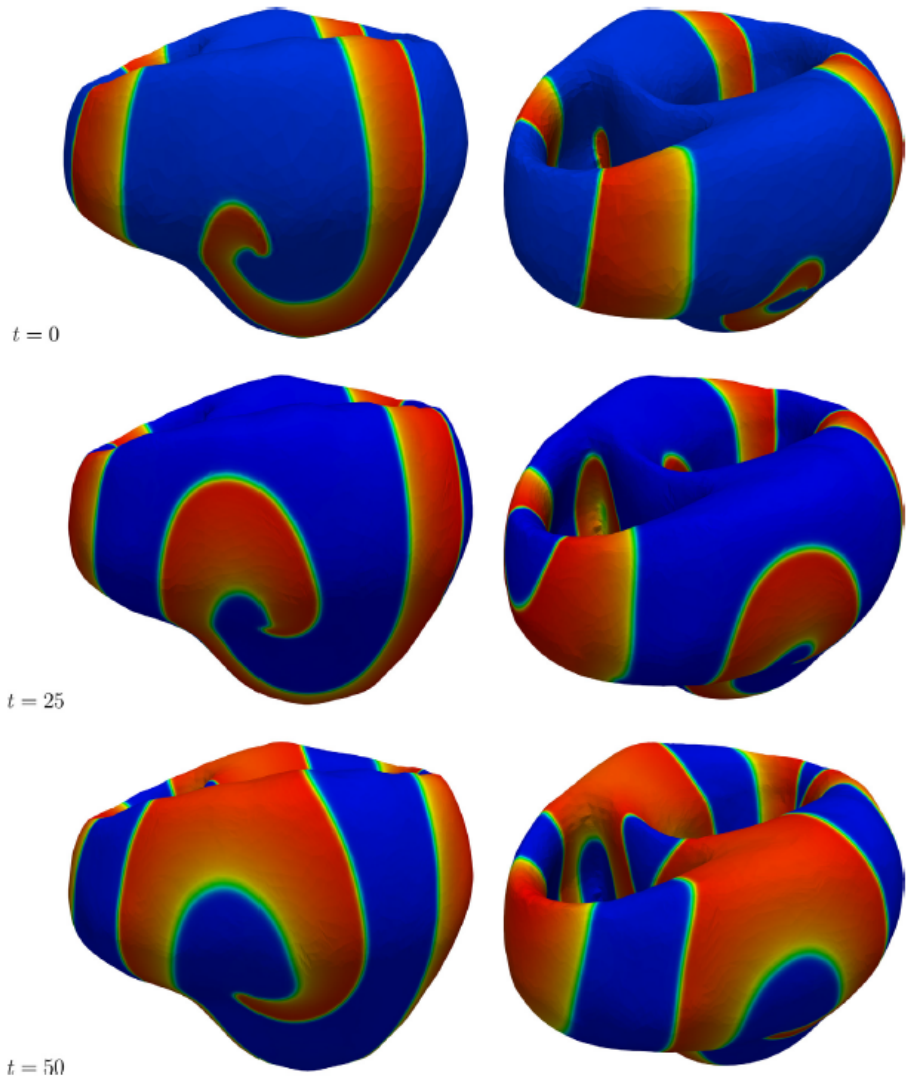

Heart geometry*

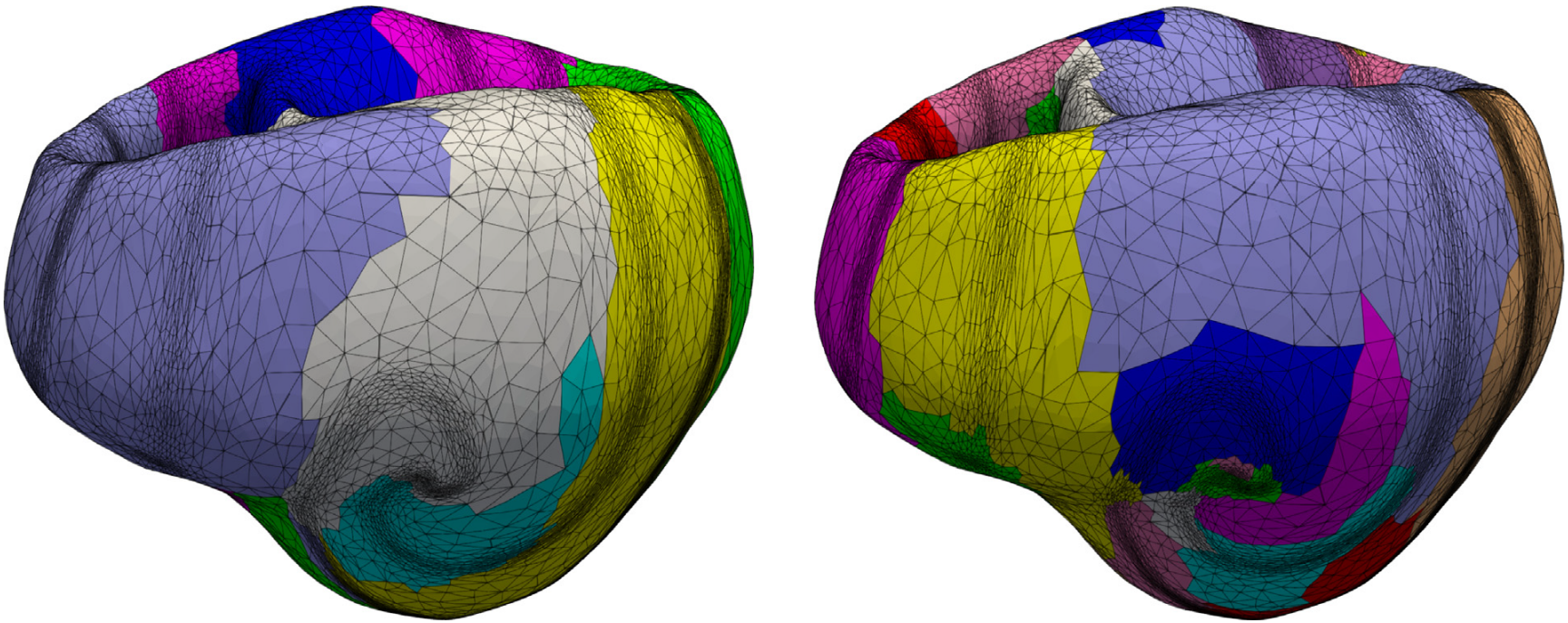

*Y. Belhamadia, T. Briffard, and A. Fortin, Efficiency of parallel anisotropic mesh adaptation for the solution of the bidomain model in cardiac tissue. Journal of Computational Science, 61, 2022

Heart geometry

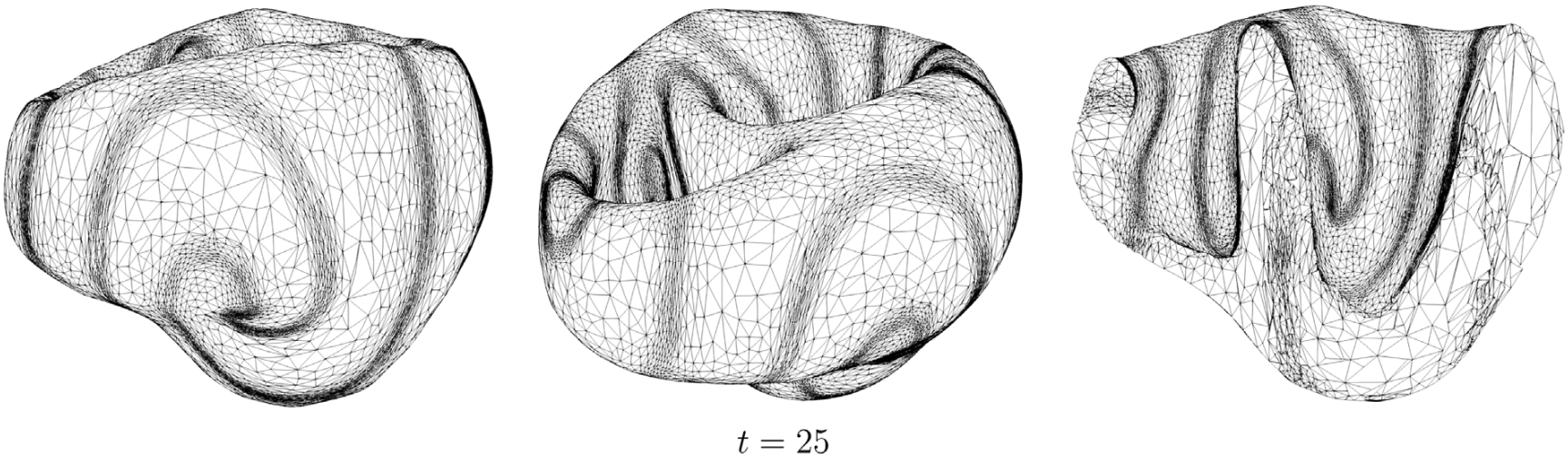

$t = 25$

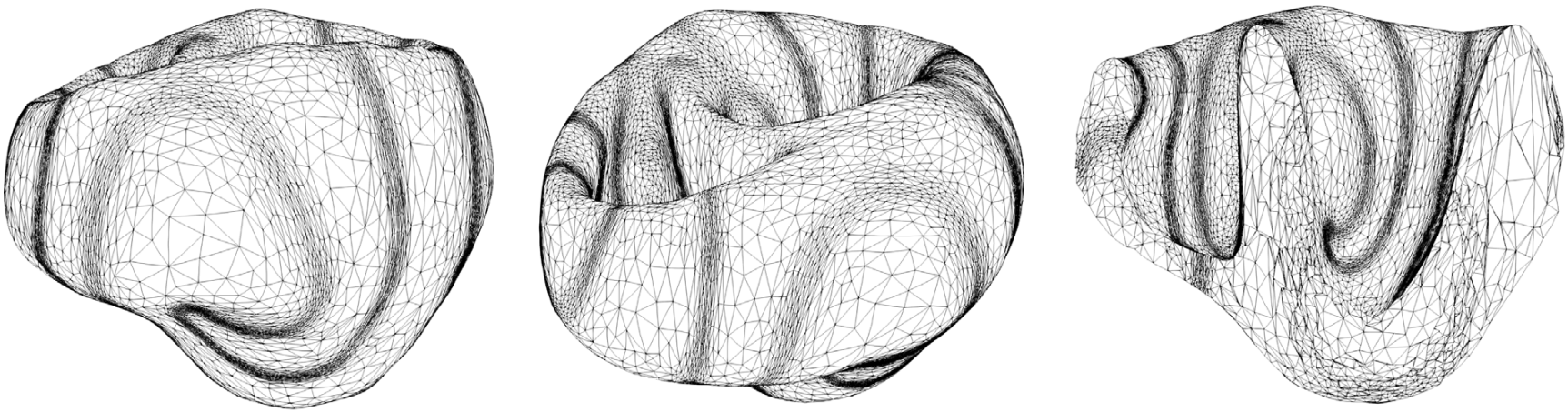

$t = 50$

Heart geometry*

Comparison of CPU time per time-step needed for the three-dimensional case: uniform mesh of size 8.1×10^6 (Mesh5) tetrahedral elements vs adapted mesh with an average of 8.4×10^4 (MeshA) tetrahedral elements.

Parallel uniform meshes				
Number of tetrahedral	CPU time 4 processors	CPU time 8 processors	CPU time 16 processors	CPU time 32 processors
8.1×10^6 (Mesh5)	49.79 min	26.67 min	13.84 min	6.93 min
Parallel adapted meshes				
8.4×10^4 (MeshA)	6.33 min	3.78 min	2.64 min	1.69 min

*Y. Belhamadia, T. Briffard, and A. Fortin, Efficiency of parallel anisotropic mesh adaptation for the solution of the bidomain model in cardiac tissue. Journal of Computational Science, 61, 2022

Coupling thermal and electrical cardiac models

$$\frac{\partial V_m}{\partial t} - \nabla \cdot (\boldsymbol{G}_i \nabla V_m) = \nabla \cdot (\boldsymbol{G}_i \nabla \phi_e) + I_{ion}(V_m, W_n),$$

$$\nabla \cdot ((\boldsymbol{G}_i + \boldsymbol{G}_e) \nabla \phi_e) = -\nabla \cdot (\boldsymbol{G}_i \nabla V_m),$$

$$\frac{\partial W_n}{\partial t} = g(V_m, W_n).$$

$$\rho c_p \frac{\partial T}{\partial t} = \nabla \cdot (k \nabla T) + b_c(T^* - T) + p_i + p_e.$$

$$p_i = j_i \cdot (-\nabla \phi_i) \quad \text{and} \quad p_e = j_e \cdot (-\nabla \phi_e).$$

$$j_i = -\boldsymbol{G}_i \nabla \phi_i \quad \text{and} \quad j_e = -\boldsymbol{G}_e \nabla \phi_e.$$

Coupling thermal and electrical cardiac models

$$\chi C_m \frac{\partial V_m}{\partial t} - \nabla \cdot (\boldsymbol{G}_i \nabla V_m) = \nabla \cdot (\boldsymbol{G}_i \nabla \phi_e) - \chi I_{ion}(V_m, W, T),$$

$$\nabla \cdot ((\boldsymbol{G}_i + \boldsymbol{G}_e) \nabla \phi_e) = -\nabla \cdot (\boldsymbol{G}_i \nabla V_m),$$

$$\frac{\partial W}{\partial t} = G(V_m, W, T),$$

$$\rho c_p \frac{\partial T}{\partial t} = \nabla \cdot (k \nabla T) + w_b c_b (T_a - T) + \boldsymbol{G}_i \nabla \phi_i \cdot \nabla \phi_i + \boldsymbol{G}_e \nabla \phi_e \cdot \nabla \phi_e.$$

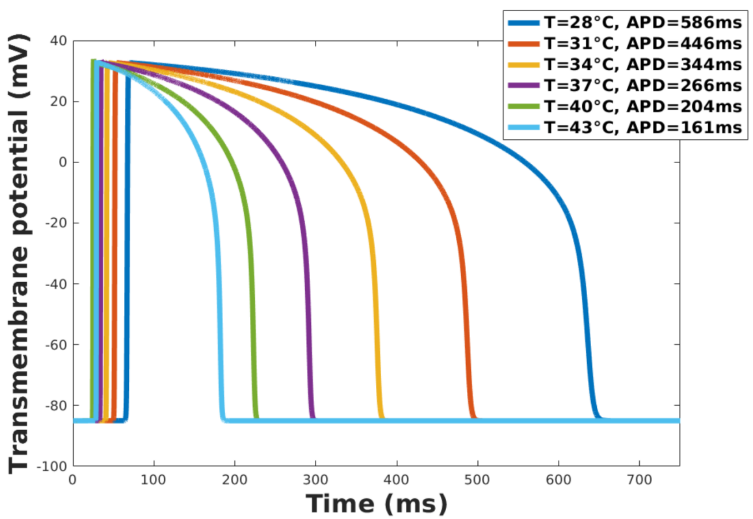

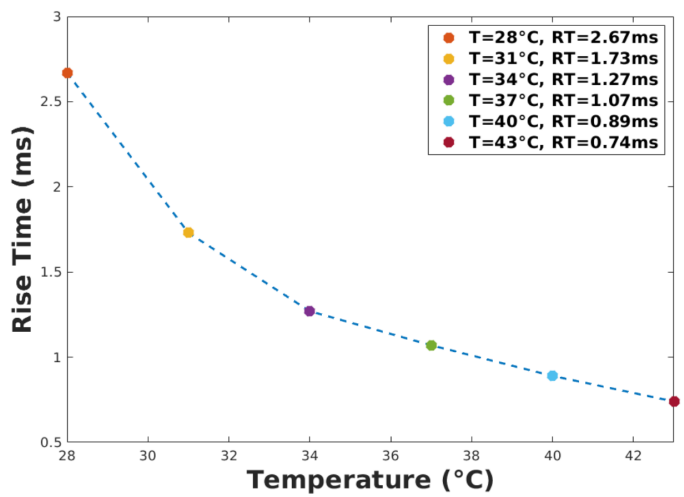

Ongoing Work

1. Coupling bidomain model with complex ionic models.
2. Coupling the mechanical and electrical cardiac models.
3. Sensibility Analysis and inverse problem.
4. Simulation of pathological cases : control of cardiac alternans.

1. Collaborations
   1. André Fortin
   2. Yves Bourgault

2. M. Alqasemi, T. Briffard, J. Grenier, and Z. Rammal.

3. Acknowledgment